

Phosphorus Analogues of Diazonium Ions. 2. Protonation of N₂, PN, and P₂

Rainer Glaser,* Christopher J. Horan, and Paul E. Haney

Department of Chemistry, University of Missouri, Columbia, Missouri 65211

Received: August 31, 1992

The potential energy surfaces of protonated N₂, P₂, and PN are explored at RHF, MP2, and CISD levels. Stationary structures were not only optimized but also characterized by computation of their vibrational frequencies at each of these levels. Model dependencies of potential energy surface characteristics, geometries, vibrational frequencies, relative isomer stabilities, and proton affinities are studied in a systematic fashion. The potential energy surface of HP₂⁺ exhibits dramatic model dependencies and it is clarified by a scan of the potential energy surface as a function of the H-P-P angle at the CISD level. Geometries and vibrational frequencies of the most stable isomers also are reported at the CISD(full)/6-311G(df,p) level. Accurate scale factors for bond lengths and vibrational frequencies determined for the neutral diatomics X≡X can be applied successfully to the protonated species as well. End-on protonation of N₂, edge-on protonation of P₂, and N-protonation of PN are favored, and our best estimates for the proton affinities are 116.3, 161.2, and 194.2 kcal/mol, respectively. Proton affinities parallel the increase of the polarizabilities (N₂ < NP < P₂) but the polarizabilities perpendicular to the bond axis, α_{perp}, are significantly smaller than α_{para} and their ratio α_{para}/α_{perp} is not related to the isomer preference energies. For protonated N₂ and P₂, the isomer preference is closely related to the X₂ bond length per se and the structural preferences of the protonated systems thus reflect the same factors that also determine the X≡X bond lengths in the neutral diatomics. The proton is atypically electrophilic compared to carbenium ions and the carbenium ion affinities of N₂, P₂, and PN are generally much smaller than proton affinities. While the potential energy surfaces of protonated and methylated N₂ and PN are qualitatively similar, the respective derivatives of P₂ differ significantly.

Introduction

The study of molecules with multiple bonds between the group V elements N and P has received increasing attention in recent years both from experimental and theoretical chemists.² One of the most fundamental questions concerns the feasibility of electrophilic attack on the triple bonds in N₂, PN, and P₂, or, in other words, the chemistry of diazonium ions and their P analogues. The formal replacement of N by P in diazonium ions I may lead to the ions II-IV or bridged isomers thereof. Aromatic



diazonium ions are well known and several of the much less stable alkyldiazonium ions³ also have been characterized in superacid media,⁴ in the gas phase,⁵ and with theoretical methods.⁶⁻¹⁰ While the experimental gas-phase data allow one to judge the quality of calculated energies, experimentally determined structural data remains scarce. Alkyldiazonium ions have been stabilized by complexation to transition metals, but in these complexes the diazonium ion is bent and it differs greatly from the free ion.^{11,12} Our recent X-ray structure determination of the β,β-diethoxyvinylidiazonium hexachloroantimonate¹³ represents the first solid state structure of any alkenediazonium ion while the C_β-N and C_β-P analogues¹⁴ have been known. Diphosphonium ions II are still elusive and, in fact, there are only a few compounds known that contain triply bonded P₂.¹⁵ Of the PN derivatives, two aromatic representatives of III have been reported by Niecke et al., namely the systems [(*t*-butyl)₂PSe₂](PNAr)¹⁶ and AlCl₄-(PNAr)¹⁷ (Ar = 2,4,6-*t*-butylphenyl), while aliphatic derivatives of III and IV remain unknown to date.

Theoretical studies of the smallest alkyl derivatives of I-IV, the methyl derivatives, strongly suggest that the analogues II-IV of diazonium ions might be synthetically accessible.¹⁸ Because of the still very limited availability of experimental data in this area, we were concerned about the adequacy of the theoretical levels employed—up to MP4(fc,sdtq)/6-311G(df,p)//MP2(fu)/

6-311G(df,p). For this reason, it seemed mandated to investigate the dependency of the results on the theoretical model and we chose to study the smaller protonated systems at higher levels of ab initio theory. In this article, we report on the systems I-IV, where R = H, the protonated species 1-4. Stationary structures on the potential energy surfaces were located and characterized by computation of the Hessian matrices at several levels up to CISD(full)/6-311G(df,p). We describe the results of our potential energy surface analyses with regard to isomer preferences and isomerizations, report the geometries of pertinent stationary structures, discuss proton affinities, and predict vibrational frequencies and other spectroscopic properties. The performances of the RHF, MP2, and CISD methods are analyzed systematically with regard to the accuracy of geometries and spectroscopic data and are discussed in comparison to the respective results for the diatomic molecules, for which experimental data exist. Comparisons to the results of prior ab initio and experimental studies of the protonated systems also are made.

Computational Methods

Geometries of HX₂⁺ were optimized for the C_{∞v} symmetric linear and C_{2v} symmetric bridged structures at the RHF, MP2-(full), and CISD(full) levels with the 6-31G* basis set¹⁹ and the resulting stationary structures were confirmed by computation of the Hessian matrix. If both of these structures corresponded to minima, then the C_s symmetric transition state structure also was determined. For the HP₂⁺ system, the potential energy surface was examined with CISD(full,6-31G*) optimized structures along a path for varying ∠(H-P-P) angles and with full characterization of all stationary structures encountered. Gradient optimizations were used at the RHF and MP2 levels, and the Fletcher-Powell method was used for the CISD optimizations. In a few instances (N₂, C_{2v} HN₂⁺), the FP method failed and the ENONLY method was used successfully instead. The most stable protonated structures of N₂, PN, and P₂ were studied also at the levels CISD(fc) and CISD(full) with the valence trip-ζ basis set 6-311G augmented by first-order polarization functions on all

TABLE I: Energies^a

method	energy	VZPE	energy	VZPE	energy	VZPE
	1, HN₂⁺, C_{∞v}		1, HN₂⁺, C_{2v}		2, HP₂⁺, C_s	
RHF/6-31G*	-109.131 930	11.33 (0)	-109.052 118	7.08 (1)		
MP2/6-31G*	-109.452 168	9.91 (0)	-109.365 304	6.08 (1)		
CISD/6-31G*	-109.431 804	10.59 (0)	-109.348 429	6.59 (1)		
SCC	-109.460 115		-109.376 207			
CISD(fc)/6-311G(df,p)	-109.501 546					
SCC	-109.530 133					
CISD/6-311G(df,p)	-109.533 344	10.82 (0)				
SCC	-109.566 334					
	2, HP₂⁺, C_{∞v}		2, HP₂⁺, C_{2v}			
RHF/6-31G*	-681.651 854	5.16 (1)	-681.670 850	5.35 (0)		
MP2/6-31G*	-681.895 156	4.87 (0)	-681.899 601	5.47 (0)	-681.878 476	4.43 (1)
CISD/6-31G*	-681.888 626	4.85 (1)	-681.902 437	5.32 (0)		
SCC	-681.924 689		-681.935 054			
CISD(fc)/6-311G(df,p)			-681.973 105			
SCC			-682.003 304			
CISD/6-311G(df,p)			-682.192 182	5.57 (0)		
SCC			-682.246 582			
	3, HNP⁺, C_{∞v}		HPN⁺, C_s		4, HPN⁺, C_{∞v}	
RHF/6-31G*	-395.446 074	10.12 (0)			-395.273 046	5.98 (1)
MP2/6-31G*	-395.731 243	9.03 (0)	-395.553 689	5.12 (1)	-395.601 007	6.23 (0)
CISD/6-31G*	-395.717 150	9.55 (0)			-395.562 086	5.54 (1)
SCC	-395.748 535				-395.603 989	
CISD(fc)/6-311G(df,p)	-395.780 254					
SCC	-395.809 078					
CISD/6-311G(df,p)	-395.913 507	9.66 (0)				
SCC	-395.957 272					

^a Total energies in atomic units and vibrational zero-point energies; VZPE, unscaled in kcal/mol. The number of imaginary frequencies, NIMAG, is given in parentheses after VZPE values.

TABLE II: Energies of Diatomics^a

method	PP		PN		NN	
	energy	VZPE	energy	VZPE	energy	VZPE
RHF/6-31G*	-681.424 535	1.30	-395.125 750	2.27	-108.943 949	3.94
MP2/6-31G*	-681.664 697	1.03	-395.430 212	1.65	-109.261 574	3.16
CISD/6-31G*	-681.655 619	1.20	-395.402 035	2.05	-109.239 421	3.57
SCC	-681.688 903		-395.436 932		-109.266 334	
CISD(fc)/6-311G(df,p)	-681.710 088		-395.460 901		-109.301 997	
SCC	-681.740 518		-395.493 344		-109.329 317	
CISD/6-311G(df,p)	-681.928 487	1.24	-395.587 871	2.13	-109.337 575	3.61
SCC	-681.982 799		-395.635 732		-109.369 514	

^a Total energies in atomic units and VZPE unscaled in kcal/mol.

atoms and with additional sets of second-order f-type functions on all heavy atoms, 6-311G(df,p).²⁰ Vibrational frequencies were determined analytically at the RHF and MP2 levels and numerically at the CISD(full) levels. All ab initio calculations were carried out with Gaussian90 and earlier versions.²¹

Results and Discussion

Total energies and vibrational zero-point energies are summarized in Table I for ions 1–4 and in Table II for the neutral diatomics. Structures are given in Table III, vibrational frequencies and IR intensities are reported in Table IV, and proton affinities are listed in Table V.

Diatomic Molecules. The experimental bond lengths of N₂, PN, and P₂ are 1.0975 Å,²² 1.4910 Å,²³ and 1.893 Å,²⁴ respectively, and their experimental vibrational frequencies are 2359.6 cm⁻¹ (¹Σ_g⁺),²⁵ 1337.0 (¹Σ⁺), and 780.8 cm⁻¹ (¹Σ_g⁺), respectively. Prior studies^{26–28} of P₂ were recently summarized by Schmidt and Gordon,²⁹ and earlier studies of PN also appeared in the literature.^{30,31}

In Table VI, the scale factors are given that are necessary to match the computed bond lengths and frequencies with the experimental values. Generally, bond lengths are *overestimated* at the RHF level and they are *underestimated by about the same amount* at the MP2/6-31G* level. All of the CISD optimized structures are in excellent agreement with experimental data and an equally good agreement can be obtained with (the more

efficient) MP2(full) optimizations with more flexible basis sets. We have used the latter finding in our studies of the P analogues of methyldiazonium ion.¹⁸ The scale factors for the vibrational frequencies reflect the same consistent trends. The underestimation at the MP2 level does show a moderate reduction with the basis set (e.g., polar PN). In the case of P₂, for example, ν (RHF) remains 36.1 cm⁻¹ too high *after* the usual scaling (factor 0.9) while, on the contrary, the unscaled frequency computed at the best MP2 level is too low (without scaling) by about the same amount (44.4 cm⁻¹).

Potential Energy Surface Analysis. Protonation of X₂. The ion HN₂⁺ was observed not only in interstellar space,³² but also in the laboratory as an intermediate in the NH₃ diazotization by Olah et al.³³ Transition metal complexes containing protonated dinitrogen ligands also are thought to be important intermediates in the reduction of elemental nitrogen.³⁴ For 1 and 2, optimized structures for end-on and edge-on protonation were determined at the levels RHF, MP2(full), and CISD(full) with the 6-31G* basis set. At all levels, end-on protonation is favored for 1 in agreement with earlier studies of the linear^{35–37} and the symmetrically bridged structures.^{38,39} In contrast, edge-on protonation is favored for the P-analogue 2 (Figure 1). The studies by Busch et al.⁴⁰ and Nguyen et al.⁴¹ also suggested that HP₂⁺ shows a modest preference for the bridged structure.

The symmetrically bridged structure of 1 is the transition-state structure for automerization. Model dependencies occur

TABLE III: Structures of HN_2^+ , HP_2^+ , and HNP^+

molecule	parameters	6-31G*			6-311G(df,p)	
		RHF	MP2	CISD	CISD(fc)	CISD
X_2	N-N	1.0784	1.1300	1.1057	1.0916	1.0898
	P-P	1.8595	1.9324	1.8913	1.8795	1.8705
HN_2^+ , $C_{\infty v}$	N-P	1.4550	1.5357	1.4873	1.4767	1.4720
	N-N	1.0709	1.1231	1.0984	1.0863	1.0841
HN_2^+ , C_{2v}	N2-H	1.0253	1.0421	1.0360	1.0316	1.0271
	N-N	1.0991	1.1491	1.1274		
HP_2^+ , $C_{\infty v}$	N1-H	1.2662	1.2890	1.2793		
	N1-N2-H	64.28	63.53	63.86		
	N2-H-N1	51.44	52.94	52.29		
	P-P	1.8351	1.9184	1.8730		
HP_2^+ , C_{2v}	P2-H	1.3916	1.4142	1.4083		
	P-P	1.9053	1.9630	1.9357	1.9261	1.9173
HNP^+ , C_s	P1-H	1.5832	1.5966	1.5947	1.5882	1.5826
	P1-P2-H	53.01	52.07	52.63	52.57	52.72
	P2-H-P1	73.98	75.87	74.73	74.66	74.57
	P-P		1.9450			
HPN^+ , C_s	P1-H		2.5443			
	P2-H		1.4331			
	P1-P2-H		96.56			
	N-P	1.4316	1.4882	1.4593	1.4493	1.4455
HPN^+ , C_s	N-H	1.0021	1.0230	1.0148	1.0067	1.0084
	N-P		1.5022			
HPN^+ , $C_{\infty v}$	P-H		1.4515			
	N-P-H		98.64			
	N-P	1.4463	1.5663	1.4867		
	P-H	1.4036	1.4329	1.4214		

^a In angstroms and degrees.

TABLE IV: Vibrational Frequencies and Infrared Intensities

	RHF/6-31G*		MP2(full)/6-31G*		CISD(full)/6-31G*		CISD(full)/6-311G(df,p)	
	ν	int	ν	int	ν	int	ν	int
NN	2758.0 (σ_g)		2179.6 (σ_g)		2497.8 (σ_g)		2528.2 (σ_g)	
PP	907.8 (σ_g)		717.0 (σ_g)		836.1 (σ_g)		868.8 (σ_g)	
NP	1588.8 (σ)	0.2	1157.3 (σ)	7.8	1436.9 (σ)	0.0	1488.2 (σ)	1.3
HNN ⁺	806.1 (π)	169.7	694.6 (π)	157.6	732.5 (π)	161.4	776.8 (π)	167.2
$C_{\infty v}$	2674.9 (σ)	12.2	2139.4 (σ)	4.2	2440.6 (σ)	4.7	2467.7 (σ)	4.0
	3639.0 (σ)	750.0	3402.7 (σ)	632.1	3501.5 (σ)	661.0	3544.6 (σ)	670.4
HNN ⁺	-837.0 (b_2)	12.9	-660.4 (b_2)	339.4	-878.9 (b_2)	25.7		
C_{2v}	2362.4 (a_1)	636.7	2027.8 (a_1)	124.1	2246.3 (a_1)	445.0		
	2588.4 (a_1)	0.0	2227.2 (a_1)	489.4	2366.8 (a_1)	127.1		
HPP ⁺	-203.6 (π)	91.1	96.3 (π)	63.7	-200.8 (π)	77.9		
$C_{\infty v}$	915.3 (σ)	13.3	702.8 (σ)	5.2	831.7 (σ)	8.2		
	2692.3 (σ)	163.2	2512.4 (σ)	117.3	2562.6 (σ)	116.8		
HPP ⁺	849.6 (a_1)	3.0	703.4 (a_1)	0.8	781.9 (a_1)	1.9	813.3 (a_1)	2.0
C_{2v}	914.4 (b_2)	70.6	1255.7 (b_2)	167.3	1044.5 (b_2)	95.2	1152.6 (b_2)	80.1
	1977.3 (a_1)	1.9	1869.7 (a_1)	14.0	1893.0 (a_1)	3.7	1931.6 (a_1)	23.6
HPP ⁺			-501.1 (a')	139.0				
C_s			726.1 (a')	30.6				
			2372.6 (a')	60.9				
HNP ⁺	792.2 (π)	230.1	706.0 (π)	193.9	740.9 (π)	204.2	743.0 (π)	191.1
$C_{\infty v}$	1624.0 (σ)	15.6	1307.1 (σ)	3.4	1489.1 (σ)	2.8	1531.1 (σ)	3.4
	3871.3 (σ)	516.4	3957.5 (σ)	439.4	3708.9 (σ)	435.9	3738.8 (σ)	467.6
HPN ⁺			-767.7 (a')	249.7				
C_s			1359.8 (a')	100.3				
			2224.4 (a')	340.3				
HNP ⁺	-220.8 (π)	69.5	492.1 (π)	8.6	-167.6 (π)	62.7		
$C_{\infty v}$	1585.0 (σ)	9.9	987.3 (σ)	78.0	1406.3 (σ)	19.0		
	2602.5 (σ)	292.9	2385.2 (σ)	132.8	2471.2 (σ)	190.1		

^a Frequencies in 1/cm, IR intensities in kilometers per mol, km/mol.

regarding the character of the linear structure of **2** and we will examine the shape of the dashed curve shown for **2** in Figure 1 in more detail below. At the RHF and CISD levels, linear **2** is a transition-state structure. At the RHF level, we established that linear **2** is in fact the transition state for the "isomerization" of bridged **2** and first it seemed reasonable to assume this to be also true at the CISD level. At the MP2 level, linear **2** is predicted to be a local minimum separated from the symmetrically bridged structure by a C_s symmetric transition-state structure which is significantly higher in energy than linear **2** (10.5 kcal/mol).

Protonation of PN. N protonation of PN resulting in linear **3** is greatly favored at all levels. Its isomer **4** is predicted to be a transition-state structure at the RHF and CISD levels. The MP2 prediction again deviates in that linear **4** is a local minimum at this level. The C_s symmetric transition state structure separating **3** and **4** on the MP2 potential energy surface was located and it is 39.7 kcal/mol less stable than **4**. At our highest level, CISD(full,ssc)/6-31G* and including vibrational zero-point energies calculated at this level, N protonation is preferred over P protonation by 86.7 kcal/mol. Maclagan⁴² recently reported

TABLE V: Proton Affinities^{a-c}

method	$C_{\infty v}$			C_{2v}		preference ^b	
	PE	$\Delta VZPE$		PE	$\Delta VAPE$	ΔPE	ΔPA^c
			N_2				
RHF/6-31G*	117.96	-7.39		67.88	-3.14	50.08	45.84
MP2/6-31G*	119.60	-6.75		65.09	-2.92	54.51	50.68
CISD/6-31G*	120.72	-7.02		68.40	-3.02	52.32	48.32
SCC	121.60			68.95		52.65	48.65
CISD(fc)/6-311G(df,p)	125.22						
SCC	126.01						
CISD/6-311G(df,p)	122.85	-7.21					
SCC	123.51						
			P_2				
RHF/6-31G*	142.64	-3.86		154.57	-4.05	-11.92	-11.73
MP2/6-31G*	144.62	-3.84		147.40	-4.44	-2.79	-2.19
CISD//6-31G*	146.21	-3.65		154.88	-4.12	-8.67	-8.20
SCC	147.96			154.46		-6.50	-6.03
CISD(fc)/6-311G(df,p)				165.05			
SCC				164.90			
CISD/6-311G(df,p)				165.47	-4.33		
SCC				165.53			
			NP				
	N-Prot	N-Prot		P-Prot	P-Prot		
RHF/6-31G*	201.01	-7.85		92.43	-3.71	108.58	104.44
MP2/6-31G*	188.90	-7.38		107.18	-4.58	81.72	78.92
CISD/6-31G*	197.74	-7.50		100.43	-3.49	97.30	93.29
SCC	195.53			104.83		90.70	86.89
CISD(fc)/6-311G(df,p)	200.40						
SCC	198.13						
CISD/6-311G(df,p)	204.34	-7.54					
SCC	201.77						

^a Values in kcal/mol. ^b Preference energies are given for end-on protonation for X_2 and for N protonation of NP. ^c $\Delta PA = (PE + \Delta VZPE)_{linear} - (PE + \Delta VZPE)_{bridged}$ for end-on protonation for X_2 and $\Delta PA = (PE + \Delta VZPE)_{N-Prot} - (PE + \Delta VZPE)_{P-Prot}$.

TABLE VI: Scale Factors for N_2 , PN, and P_2

method	bond length			frequency		
	NN	PN	PP	NN	PN	PP
RHF/6-31G*	1.02	1.02	1.02	0.86	0.84	0.86
MP2/6-31G*	0.97	0.97	0.98	1.08	1.16	1.09
MP2/6-311G*	0.98	0.98	0.98	1.08	1.13	1.09
MP2/6-311G(df)	0.99	0.98	0.99	1.07	1.11	1.06
CISD/6-31G*	0.99	1.00	1.00	0.94	0.93	0.93
CISD(fc)/6-311G(df)	1.01	1.01	1.01			
CISD/6-311G(df)	1.01	1.01	1.01	0.93	0.90	0.90

^a Scale factor = experimental value/computed value.

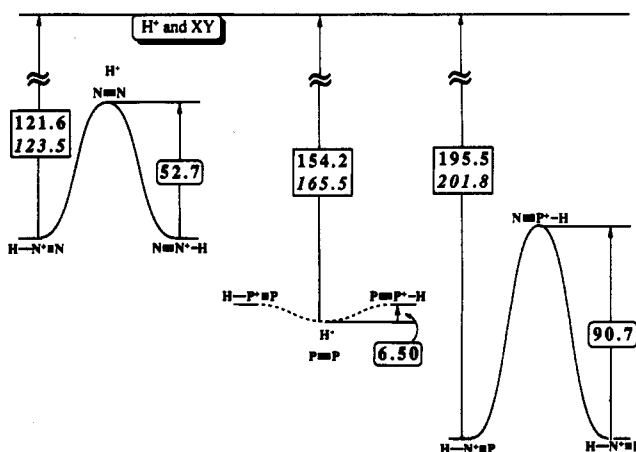


Figure 1. Schematic drawings of the potential energy surfaces of protonated N_2 , PN, and P_2 . Energy profiles are drawn to scale vertically and the energies given are those determined at the CISD(full)/6-31G* level (without VZPEs). Values given in italics were determined at the CISD(full)/6-311G(df,p) level.

proton affinities of phosphorus compounds including PN. $(HNP)^+$ was found to be preferred over HPN^+ by 91.7 kcal/mol at MP4-

(sdq)/6-31G*/RHF/6-31G*. This is also in agreement with the earlier MRD-CI study with double- ζ plus polarization basis sets by Buenker et al.⁴³ that showed HNP^+ to be favored over HPN^+ by 87.4 kcal/mol and that the latter is a transition state structure.

The most stable structures resulting from protonation of N_2 , PN, and P_2 , respectively, linear 1, C_{2v} 2, and linear 3 were optimized also at CISD(full)/6-311G(df,p) and confirmed to be minima at that level (Table IV). Before we proceed to discussing relevant properties of the stationary structures obtained, we address some pertinent aspects of model dependencies.

Model Dependencies. At the MP2(full)/6-31G* level, the stationary structures of linear 2 and 4 are predicted to be local minima rather than transition state structures. These results suggest that P σ lone pair dative bonding to electrophiles is artificially overestimated at the MP2/6-31G* level. This artifact may formally be viewed either as originating from an artificial stabilization of the linear structures or as an artificial destabilization of the structures in their vicinities on the potential energy surfaces. Considering the relatively close agreement of the relative energies of end-on and edge-on coordinated structures (Table V), the latter seems to be more important; that is, the activation associated with the change from end-on to edge-on coordination is artificially enhanced. We will present compelling evidence for this conclusion (a) by showing that model dependencies on the linear structures are modest and (b) by exploration of the potential energy surface at the CISD(full)/6-31G* level along the H-P-P path.

Basis Set Dependencies in the MP2 Calculations of $H-P^+ \equiv X$. We studied linear 2 and 4 also with valence triple- ζ basis sets with different choices of polarization functions to examine whether these deficiencies are basis set dependent. Both molecules were optimized and characterized at the MP2(full) level with the 6-311G(d,p), 6-311G(dd,p), and the 6-311G(df,p) basis sets and the results are summarized in Table VII. Basis set effects on

TABLE VII: MP2(full) Optimized Structures of Linear HPP⁺ and HPN⁺

basis set	energy	VZPE	H-P	P-X	$\nu(\pi)$	$\nu(\sigma)$	$\nu(\sigma)$
			HPP ⁺				
6-311G(d,p)	-682.174 436	5.03	1.4045	1.9084	146.7	706.6	2515.1
6-311G(dd,p)	-682.219 592	5.01	1.4062	1.9193	167.5	692.6	2474.3
6-311G(df,p)	-682.211 516	4.61	1.4083	1.9037	-38.3	724.3	2502.1
			HPN ⁺				
6-311G(d,p)	-395.780 763	6.21	1.4227	1.5570	474.2	1004.9	2389.6
6-311G(dd,p)	-395.299 236	6.08	1.4281	1.5565	463.9	997.4	2328.0
6-311G(df,p)	-395.814 828	6.06	1.4306	1.5509	429.0	1031.0	2351.7

structures are found to be modest. All bonds are slightly shortened and the agreement with the CISD optimized structures is improved. The variations in the low-energy vibrational π -symmetric modes are most diagnostic. For linear 2, optimization of the d-function exponent through linear combination of two sets of d-type polarization functions increases $\nu(\pi)$ but this mode becomes imaginary when sets of first- and second-order polarization functions are used. For linear 4, improvements in the basis set results in the same trends but the activation barrier persists. Interestingly, the small contributions of the f-type functions suffices to change the character of linear 2 from a minimum to a transition state. Could this small change in the theoretical model remove the barrier for end-on to edge-on isomerization and cause linear 2 itself to become the transition-state structure? We thus determined the potential energy surface of 2 as a function of the H-P-P angle to clarify this question.

CISD Potential Energy Surface Scan for H-P⁺≡P. The results of our exploration of the potential energy surface of 2 at the CISD(full)/6-31G* level are summarized in Table VIII and graphically illustrated in Figure 2. The potential energy scan at the CISD level (solid circles in Figure 2), unexpectedly revealed two more stationary structures in addition to the symmetrically bridged and linear structures and both of these were optimized and characterized by calculation of their vibrational frequencies. A local minimum occurs at an H-P-P angle of 147.1° and it is only slightly more stable than the transition state structure linear 2; the activation barrier is 0.39 kcal/mol at the level of optimization and 0.64 kcal/mol with inclusion of corrections for size consistency (+0.52 kcal/mol) and vibrational zero-point energies (-0.27 kcal/mol). At an H-P-P angle of 108.2°, a transition-state structure occurs for an asymmetrically bridged structure of 2. This transition-state structure is 0.67 kcal/mol less stable than the adjacent local minimum at the CISD/6-31G* level and with inclusion of corrections for size-consistency (+0.01 kcal/mol) and vibrational zero-point energies (-0.52 kcal/mol) the barrier becomes 0.16 kcal/mol. Thus, the essential features of the potential energy surface of HP₂⁺ are (a) that the symmetrically bridged structure is the most stable one, (b) that displacements of the hydrogen from the symmetrically bridging position lead to a sharp increase in energy, and that (c) the variation in energy in the entire region of the potential energy surface where 90° < H-P-P < 270° is within 1 kcal/mol.

In Figure 2, also shown are the potential energy curves calculated at the RHF, MP2, and MP3 levels with the CISD optimized structures which provide excellent approximations to the true potential energy curves at those levels. *The RHF and MP2 curves both differ most dramatically in qualitative fashions from the CISD results.* The RHF energy rises monotonically along the path from bridged 2 to linear 2. Except for a small shoulder around H-P-P = 80°, the transition from edge-on to end-on coordination occurs rather steady and without any asymmetric stationary structures along the path. On the other hand, the MP2 energies suggest a much more pronounced barrier for the transition between π -type protonation and η^1 coordination just as observed on the MP2/6-31G* surface itself (vide supra). The maximum of the MP2 energy occurs at H-P-P = 95° and would indicate a barrier of about 13 kcal/mol for the transition from bridged 2 to linear 2. Note that the MP2/6-31G* optimized

structures and energies agree very closely with these data. It is only with third-order perturbational theory that the characteristic features of the potential energy surface are reproduced (Figure 2) although the barrier between the symmetrically and asymmetrically bridged structures is somewhat overestimated.

Busch et al.⁴⁰ previously studied the potential energy surface of 2 as a function of the H-P-P angle at the RHF level. The CEPA-1 method was employed together with the RHF structures to estimate electron correlation effects. This correlation treatment leads to a lowering of the energy but not to a minimum in that area of the potential energy surface where our CISD(full)/6-31G* study indicates the asymmetrically bridged minimum.⁴⁴ Moreover, the CEPA-1/RHF calculations fail to reproduce the flatness in extended region with 90° < H-P-P < 270°.

The flatness of the potential energy surface in the region around linear 2 provides a simple explanation for the model dependency of the character of linear 2. While the potential energy surface in that vicinity is predicted to be rather flat at all levels of theory, its gradient does depend on the method's ability to describe that region of the potential energy surface in which the hydrogen changes from π - to σ -coordination.

The CISD/6-31G* optimized P-P and P-H bond lengths in symmetrically bridged 2 are 1.9357 and 1.5947 Å, respectively, and they both are shorter in linear 2 where $d(\text{P-P}) = 1.8730$ Å and $d(\text{P-H}) = 1.4083$ Å. See Table VIII for their variations along the path. The P-P bond varies comparatively little (<0.09 Å or 5%) and it goes through a maximum at an H-P-P angle of about 90°. The P-H bond shortens significantly more in going from bridged 2 (1.5947 Å) to linear 2 (1.4083 Å) and the change is essentially monotonous (except for a small bump around H-P-P = 130°).

Geometries. Lacking the possibility for direct comparison to experimental data, we elucidate model dependencies on structures by comparison to the neutral diatomics for which experimental data exist (vide supra). In Figure 3, the X-Y bond lengths are shown as a function of the theoretical level. Data indicated by an X refer to the neutral diatomics and the interpolation lines terminate at the experimental values (level 6). The X-Y bond lengths calculated for linear 1 and 3 (unfilled circles) and bridged 2 (triangles) show the same pattern over the five levels as the diatomic molecules themselves. The nonconnected unfilled (filled) circles in Figure 3 refer to linear 2 (4). Because of these great similarities, it appears reasonable to assume that the true X-Y bond lengths in the protonated systems are well bracketed by the RHF and MP2 derived bond lengths and somewhat longer than the bond distances predicted by our highest CISD level. Moreover, the spread in the structural parameters is of a comparable magnitude as for the diatomics and the scale factor discussed there can be used.⁴⁵

The CISD(full)/6-31G* optimized structures are illustrated in Figure 4 with a common scale. End-on protonation shortens the X-Y bonds in all cases. The shortening is negligible for linear 1 and 4, modest for linear 2 (0.018 Å), and most pronounced for linear 3 (0.028 Å).⁴⁶ Edge-on protonation, on the other hand, lengthens the basal X-X bonds, and the effect is more pronounced (0.022 Å for 1 and 0.044 Å for 2). All of the X-Y bonds in the protonated systems and in the diatomics differ less than 2.5%, almost a magnitude less than the changes associated with bond

TABLE VIII: CISD Optimized Structures of HPP⁺ as a Function of the H-P-P Angle^a

$\angle(\text{HPP})$	52.63 ^b	70°	80°	90°	100°	108.19 ^c	110°	130°	147.14 ^d	150°	180 ^b
P-P	1.9357	1.9400	1.9528	1.9566	1.9499	1.9392	1.9360	1.9056	1.8874	1.8850	1.8730
P-H	1.5947	1.4791	1.4514	1.4339	1.4237	1.4182	1.4170	1.4192	1.4073	1.4068	1.4083
RHF	-681.670 173	-681.664 801	-681.662 948	-681.661 985	-681.660 658	-681.659 103	-681.658 724	-681.654 538	-681.652 161	-681.651 905	-681.650 534
MP2	-681.899 193	-681.887 185	-681.881 506	-681.878 879	-681.878 531	-681.879 692	-681.880 116	-681.887 100	-681.892 230	-681.892 724	-681.893 966
MP3	-681.920 294	-681.910 304	-681.905 664	-681.903 357	-681.902 529	-681.902 704	-681.902 839	-681.905 694	-681.907 656	-681.907 780	-681.907 432
CISD	-681.902 437	-681.894 152	-681.890 639	-681.889 017	-681.888 334	-681.888 183	-681.888 190	-681.889 254	-681.889 246	-681.889 246	-681.888 626
CISD(ssc)	-681.935 054	-681.927 502	-681.924 790	-681.924 077	-681.924 421	-681.925 061	-681.925 200	-681.926 347	-681.926 141	-681.926 009	-681.924 689

^a All electrons included in CI. Basis set 6-31G*. ^b First and last data columns contain the parameters for C_{2v} and C_{∞v} structures, respectively. ^c Parameters for the transition state involving asymmetric bridging. Vibrational frequencies: -231.4 (a'), 737.5 (a'), 2480.4 (a'), 2562.3 (a'). ^d Parameters for the local minimum involving asymmetric bridging. Vibrational frequencies: 199.8 (a'), 817.9 (a'), and 2562.3 (a'). Vibrational zero-point energy: 5.12 kcal/mol.

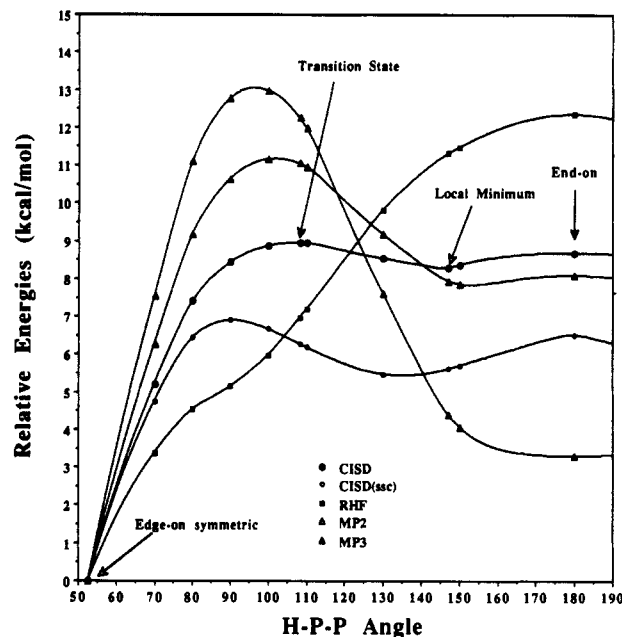


Figure 2. The potential energy surface of HP₂⁺ as a function of the H-P-P angle is shown. All energy values are based on the CISD(full)/6-31G* optimized structures for a given angle.

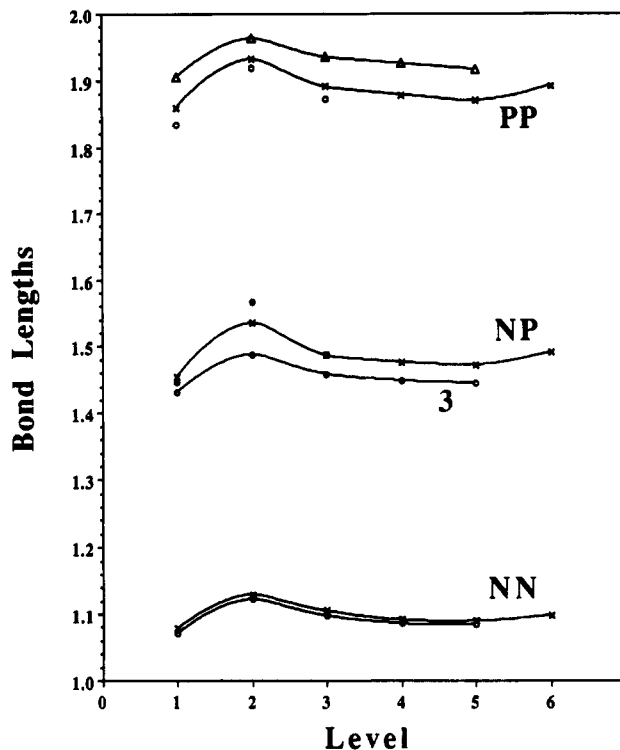


Figure 3. Effects of the theoretical model on geometries. Levels 1-5 represent RHF/6-31G*, MP2(full)/6-31G*, CISD(full)/6-31G*, CISD(fc)/6-311G(df,p), and CISD(full)/6-311G(df,p), respectively. Entries for level 6 are the experimental data.

order reduction of one. The P-N bond in 3 (1.459 Å) is 0.028 Å shorter than the one in 4 (1.487 Å). Nonetheless, the latter remains much shorter than the P-N bond length of 1.57 Å in PN⁺ in its 2Σ⁺ state (7σ e⁻ loss from PN) that was determined via Penning ionization.⁴⁷ Note that the N-P distance in 4 is greatly overestimated at the MP2/6-31G* level (1.57 Å) suggesting a much greater similarity with PN⁺. The experimental bond lengths⁴⁸ of the 2Σ⁺ (ground) states of N₂⁺ (1.116 Å) and P₂⁺ (1.893 Å) are very close to the values in the neutral molecules and, thus, they may not be taken as an indicator of the charge distribution in 1 and 2. The H-N (H-P) bond length in linear

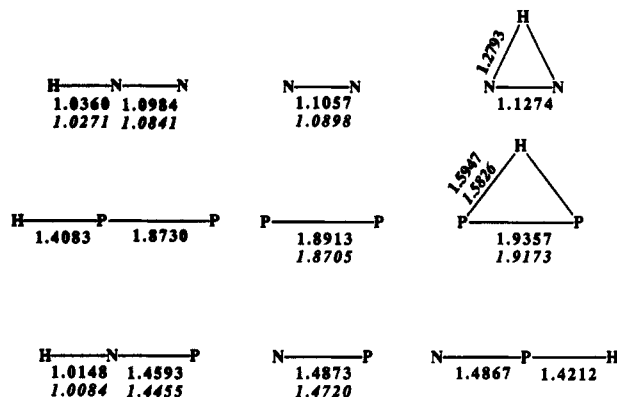


Figure 4. Drawings (to scale) of the CISD(full)/6-31G* optimized structures. Values in italics were determined at the CISD(full)/6-311G-(df,p) level for the most stable structures.

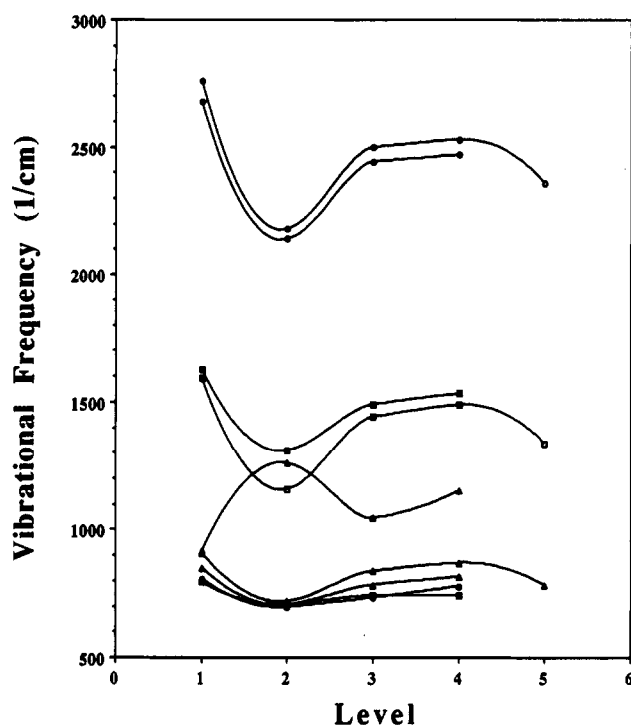


Figure 5. Effects of the theoretical model on vibrational frequencies. Levels 1–4 represent RHF/6-31G*, MP2(full)/6-31G*, CISD(full)/6-31G*, and CISD(full)/6-311G(df,p), respectively. Entries for level 5 are the experimental data for the neutral molecules.

1 (2) is 0.021 (0.013) Å shorter than in 3 (4) reflecting the higher basicity of N (P) in 1 (2) compared to 3 (4). H–X bonds in the bridged structures are longer compared to the linear structures, and more so for the 1 (0.243 Å) than for 2 (0.186 Å).

Spectroscopic Properties. Harmonic vibrational frequencies, their symmetries, and infrared intensities are given in Table IV. In Figure 5 the dependencies are graphically illustrated of the computed vibrational frequencies on the theoretical model. Unfilled circles, squares, and triangles refer to the stretching frequencies of N₂, NP, and P₂, and the corresponding filled marks indicate the lower two frequencies in linear 1⁴⁹ and 3 and in bridged 2, respectively. It becomes immediately obvious from this figure that the trends discussed for the frequency scale factors of the neutral diatomics carry over to the protonated systems. The scale factors given in Table VI for the neutral molecules also might be used for the protonated systems. The model dependency of the b₂ mode of bridged 2 stands out in that the frequency calculated at the MP2 level exceeds both the RHF and CISD values. This mode corresponds to a proton movement relative to the PP axis in a parallel fashion, and its overestimated value is

a consequence of the discussed deficiencies of the potential energy surface at this level.

With the CISD(full)/6-311G(df,p) data and the scale factors in Table VI, we predict the vibrational frequencies (1/cm) of the most stable protonated systems to be 725 (π, ν₂), 2303 (σ, ν₃), and 3308 (σ, ν₁) for linear 1, 731 (a₁), 1036 (b₂), 1736 (a₁) for bridged 2, and 668 (π), 1376 (σ), and 3359 (σ) for 3, respectively. The predicted frequencies for linear 1 can be compared to experimental data available from infrared laser spectroscopy. Gudemann et al.⁵⁰ measured a frequency ν₁ = 3234 cm⁻¹ and Foster and McKellar⁵¹ reported ν₃ = 2258 cm⁻¹. Our best estimates for ν₁ and ν₃ thus remain slightly too high by 74 and 45 cm⁻¹, respectively, but the agreement is *much* better than that obtained with standard scaling methods.⁵²

Proton Affinities. In Table V, the protonation energies PE are given for 1–4. The energies refer to the motionless state at 0 K. Proton affinities can well be approximated with the protonation energies if the changes in vibrational zero-point energies are taken into account, PA = PE + ΔVZPE. The ΔVZPE values in Table V are given unscaled. The errors associated with the ΔVZPE values may be as large as 10% (vide supra), but they remain on the order of only 0.3–0.8 kcal/mol, and these errors essentially cancel in the determination of the relative proton affinities of isomeric structures (last column Table V).

Relative Proton Affinities. At the CISD(full)/6-31G* level and including corrections for vibrational zero-point energies, preference energies of 48.7 and 6.0 kcal/mol are found for linear 1 and bridged 2, respectively. The preference energies for the linear structures, ΔPA, are larger than the RHF values and smaller than the MP2 values, that is, electron correlation tends to favor linear structures but the ΔPA values suggest that this trend is overestimated at the second-order perturbation level. Trends in the PE values provide useful insights. The PE values for linear 1 and 2 all increase monotonically with improvement in the theoretical model. The RHF and CISD PE values of bridged 1 and 2 are within less than 0.5 kcal/mol, whereas the MP2 derived PE values are significantly less and in particular for 2. The origin for the overestimated preferences for the linear structures at the MP2 level is thus not an overestimation of the correlation effects on the linear structures but rather the inadequacy of the correlation corrections to accurately approximate the electron correlation effects on the bridged species. The entries ΔPE and ΔPA for NP in Table V refer to the preference for N protonation over P protonation. At the CISD level, the N-protonation preference is 86.7 kcal/mol. Second-order corrections significantly improve the ΔPA value; ΔPA(RHF) is 17.8 kcal/mol higher while ΔPA-(MP2) is lower by 7.8 kcal/mol.

End-versus Edge-On Preference and X–X Bond Length. Ions 1 and 2 may be compared regarding their preferences for end-on or edge-on protonation and regarding the magnitudes of the interactions. The homologues 1 and 2 differ characteristically with regard to the former criterium. We optimized structures of linear and bridged 1 with fixed N–N bond distances and their energies relative to the respective stationary structures are plotted versus *d*(N–N) in Figure 6. An increase of *d*(N–N) does have a significantly larger effect on the linear structure. For the range examined, the energy increase of the linear over the bridged structure, ΔΔE, follows a quadratic function and ΔΔE reaches a value⁵³ of about 50 kcal/mol for *d*(N–N) = 1.6 Å. Note that the calculated preference for linear 1 is of about equal magnitude. On the other hand, the shorter P–P bond length results in higher destabilizations of the bridged compared to the linear structure. The structures with *d*(P–P) = 1.5 Å, for example, differ by about 40 kcal/mol with a preference for the linear structure.⁵⁴ In both cases, the bridged structure becomes destabilized relative to the linear structure with the same bond length as the X–X bond length is shortened. This finding can be rationalized with qualitative MO theory. The approach of an electrophile toward

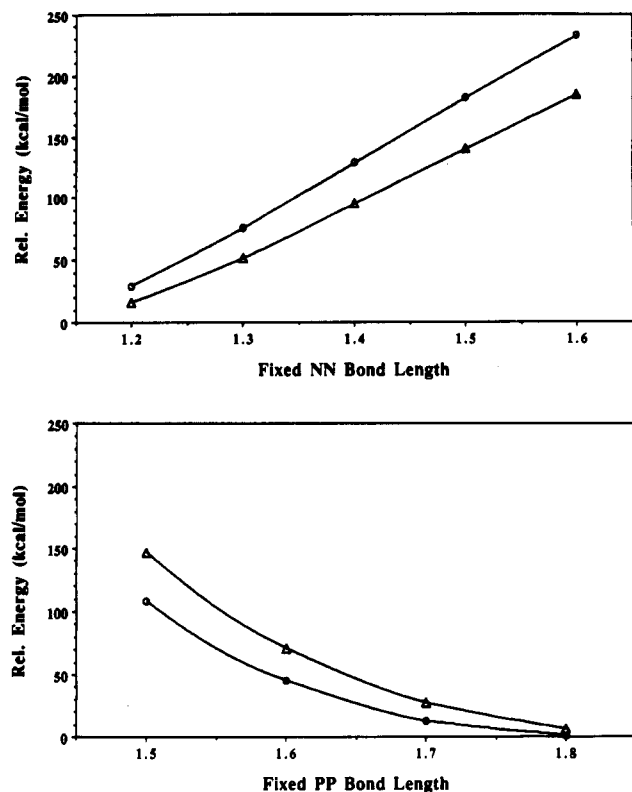


Figure 6. Bridged structures become destabilized relative to the linear structure with the same bond length as the X–X bond length is shortened. Relative energies of linear (circles) and bridged (triangles) protonated N₂ with increasing N–N distances (top) and of protonated P₂ with decreasing P–P distance.

the π system polarizes the π system to increase the bonding of the electrophile but it also leads to increased electron–electron repulsion in the π system. A longer X–X bond will allow the first effect to dominate the second whereas the second effect will dominate for shorter bonds. To a first approximation, we may disregard the small differences in the X–X bond lengths of the linear and bridged structures in 1 and 2, and conclude that *the preference for the bridged structures is closely related to the X–X bond length⁵⁵ and the structural preferences of the protonated systems thus reflect the same factors that also determine the X–X bond lengths in the neutral diatomics.*

Absolute Proton Affinities. Accurate determinations of proton affinities are difficult⁵⁶ as the combination of a proton with a nucleophile is the worse case scenario for basis set superposition errors.⁵⁷ The best remedy against such errors is the enlargement of the basis set. We determined the proton affinities of N₂ (giving linear 1), of NP (leading to 3), and of P₂ (resulting in bridged 2) at the CISD(full)/6-311G(df,p) level and including vibrational zero-point energy corrections determined at this level. Our best estimates for these proton affinities associated with the formations of 1–3 are 116.3, 161.2, and 194.2 kcal/mol, respectively. The experimental proton affinity of N₂ is 118.2 kcal/mol,⁵⁸ and it is in excellent agreement with our best theoretical value and also with other reported values⁵⁹ that included good correlation treatments. Also, the experimental proton affinity of 191.0 kcal/mol NP was recently reported⁶⁰ and it is within 3 kcal/mol of our best theoretical value.

Proton Affinities and Polarizabilities. Selected spectroscopic properties including polarizabilities for the diatomic molecules are summarized in Table IX. The polarizabilities increase in the order N₂ < NP < P₂ and this increase parallels the increase in their proton affinities. The polarizabilities perpendicular to the bond axis, α_{perp} , are significantly smaller than α_{para} and the ratio $\alpha_{\text{para}}/\alpha_{\text{perp}}$ is about the same for N₂ (2.1) and PN (1.9) but it is

TABLE IX: Spectroscopic Properties of the Diatomics

parameter	NN	NP	PP
molecular mass	14.003	16.883	30.974
RHF/6-31G*			
force constant	62.757	25.110	15.037
dipole μ	0.0	2.921	0.0
quadrupole perp	-10.182	-17.395	-26.276
quadrupole para	-11.671	-20.312	-26.977
polarizability α_{perp}	5.856	14.799	21.700
polarizability α_{para}	13.380	29.872	66.651
rotational constant	62.070	24.753	9.438
MP2/6-31G*			
force constant	39.202	13.321	9.377
dipole μ	0.0	2.289	0.0
quadrupole θ_{perp}	-10.149	-17.531	-26.000
quadrupole θ_{para}	-11.895	-20.280	-26.824
polarizability α_{perp}	6.177	15.008	21.569
polarizability α_{para}	12.999	29.166	62.732
rotational constant	56.528	22.222	8.738
MP2/6-311G*			
frequency ν_{calc}	2185.6 σ	1180.7 σ	716.8 σ
force constant	39.411	13.876	9.376
dipole μ	0.0	2.491	0.0
IR intensity	0.0	7.6	0.0
rotational constant	57.641	22.677	8.804
MP2/6-311G(df)			
frequency ν_{calc}	2208.1 σ	1204.3 σ	736.4 σ
force constant	40.227	14.427	9.895
dipole μ	0.0	2.437	0.0
IR intensity	0.0	8.0	0.0
rotational constant	58.102	22.659	8.876

* Frequencies in cm⁻¹, force constants in mdyn/Å, IR intensities in km/mol, dipole moments in debye (1 au = 2.5418 D), quadrupoles in D·Å, polarizabilities in atomic units, rotational constants in GHz.

significantly larger for P₂ (2.9). The ratios of $\alpha_{\text{para}}/\alpha_{\text{perp}}$ might have been expected to reflect the stereochemical preferences regarding end-on or edge-on coordination to an electrophile and the absolute α values may give an indication of the strength of such an interaction so long as the interaction is primarily electrostatic in nature.

Proton versus Carbenium Ion Affinities. The potential energy surfaces of protonated and methylated N₂ and PN are qualitatively similar whereas the respective derivatives of P₂ differ distinctly. Protonation leads to the bridged structure as the only minimum and the linear structure is a transition state structure. Methylation, on the other hand, results in minima for end-on and asymmetric edge-on coordination with the former being preferred.⁶¹

The proton is atypically electrophilic compared to carbenium ions because of its lack of core electrons and, for this simple reason, carbenium ion affinities are generally much smaller than proton affinities. For example, the methyl cation affinities of N₂, P₂, and NP, are 43.0, 71.3, and 100.4 kcal/mol, respectively, at MP4(fc,sdtq)/6-311G(df,p)//MP2(full)/6-311G(df,p) and including MP2(full)/6-311G(d) vibrational zero-point energies.¹⁸ The smaller affinities are accompanied by smaller structural changes to the XY units upon addition of the electrophile and smaller electronic relaxations also are indicated. Model dependencies on structures are less pronounced for these methylated systems and second-order perturbational corrections do not affect the characteristics of the potential energy surfaces.¹⁸ Caution is required nevertheless for systems with P σ lone pair dative bonds to electrophiles. For example, C_{3v} CH₃PN⁺ is a very shallow minimum on the RHF/6-31G* and MP2(full)/6-31G* potential energy surfaces and this structure might be a transition state structure.⁶² For CH₃PP⁺, the isomer preference energy might be affected to some extent as well, but the qualitative conclusions should remain valid.

Conclusion

The potential energy surfaces of protonated N_2 , P_2 , and PN all were examined at the RHF, MP2(full), and CISD(full) levels with the 6-31G* basis set. At all levels, end-on protonation of N_2 , edge-on protonation of P_2 , and N protonation of PN are favored and our best estimates for their proton affinities are 116.3, 161.2, and 194.2 kcal/mol, respectively, at CISD(full)/6-311G-(df,p) and including vibrational zero-point energy corrections determined at that level. It is emphasized that the proton affinities do not necessarily reflect the stability of these ions toward dissociation. The dissociations of 1–3 into H^+ atom and the radical cations N_2^+ ($2\Sigma^+$), P_2^+ ($2\Sigma^+$), and PN^+ (2Σ), respectively, are endothermic by 151.9, 138.9, and 74.6 kcal/mol, respectively, at the CISD(full)/6-31G* level and including vibrational zero-point energies calculated at that level.⁶³ For 2 and 3 and in contrast to 1, the homolytic dissociations are thermodynamically favored compared to deprotonation and future studies of their activation barriers will have to show whether radical formation provides for a viable reaction channel.

For protonated N_2 and P_2 , the bridged structure becomes destabilized relative to the linear structure with the same bond length as the X–X bond length is shortened. We conclude that the preference for the bridged structures is closely related to the X–X bond length per se and that the structural preferences of the protonated systems reflect the same factors that also determine the X–X bond lengths in the neutral diatomics. Because of the incompleteness of experimental structural and spectroscopic data for the protonated systems, the model dependencies of bond lengths and vibrational frequencies of the neutral diatomics, for which experimental data exist, were studied and the scale factors derived for these also appear adequate for the protonated species in light of the demonstrated close agreement of the model dependencies.

Qualitative differences between the MP2 and CISD levels occur for linear HP_2^+ and HPN^+ with regard to their characters. The understanding of these differences is important to judge the validity of MP2 derived theoretical data of larger systems for which full optimizations at the CISD level might not be feasible. Our results suggest that P σ lone pair dative bonding of the proton leads to local minima at the second-order Møller–Plesset level because of an artificial destabilization of the structures in their vicinities on the potential energy surfaces that results in an artificial activation associated with the change from end-on to edge-on coordination. Larger well polarized basis sets with second-order f-type polarization functions reduce (or even eliminate) this deficiency. With regard to isomer stabilities, the MP2 results qualitatively agree with the CISD predictions but modest quantitative differences occur. Our study suggests that the underestimation of the preference for bridged over linear HPP^+ at the MP2 level is caused by the underestimation of electron correlation effects on the bridged species rather than by an overestimation of the stability of the linear structures. Both of these features indicate that MP2 theory tends to underestimate the stabilities of bridged structures, and more so for the unsymmetrically bridged species.

Acknowledgment is made to the donors of the Petroleum Research Fund (PRF # 24399-G4), administered by the American Chemical Society, for support of this research. P.E.H. thanks the National Science Foundation for a 1991 Senior Enhancement Fellowship. R.G. thanks the National Science Foundation for a travel grant to the International Conference on Phosphorus Chemistry in Toulouse, France, and Professor Slayton A. Evans for organizing this grant.

References and Notes

(1) (a) Presented in part at the XIIth International Conference on Phosphorus Chemistry, Toulouse, France, July 1992. (b) For part I of the series, see ref 18.

- (2) *Multiple Bonds and Low Coordination in Phosphorus Chemistry*; Regitz, M.; Scherer, O., Eds.; Thieme Verlag: New York, 1990.
- (3) Reviews: (a) Kirmse, W. *Angew. Chem., Int. Ed. Engl.* **1976**, *15*, 251. (b) Laali, K.; Olah, G. A. *Rev. Chem. Intermed.* **1985**, *6*, 237.
- (4) (a) Mohrig, J. R.; Keegstra, K. *J. Am. Chem. Soc.* **1967**, *89*, 5492. (b) Mohrig, J. R.; Keegstra, K.; Mavrick, A.; Roberts, R.; Wells, S. J. *J. Chem. Soc., Chem. Commun.* **1974**, 780. (c) Avaro, M.; Levisalles, J.; Sommer, J. M. *J. Chem. Soc., Chem. Commun.* **1968**, 410. (d) McGarrity, J. F.; Cox, D. Ph. *J. Am. Chem. Soc.* **1983**, *105*, 3961.
- (5) (a) Foster, M. S.; Beauchamp, J. L. *J. Am. Chem. Soc.* **1972**, *94*, 2425. (b) Foster, M. S.; Williamson, A. D.; Beauchamp, J. L. *Int. J. Mass. Spectrom. Ion Phys.* **1974**, *15*, 429. (c) McMahon, T. B.; Heinis, T.; Nicol, G.; Hovey, J. K.; Kebarle, P. *J. Am. Chem. Soc.* **1988**, *110*, 7591.
- (6) Glaser, R. *J. Phys. Chem.* **1989**, *93*, 7993.
- (7) Glaser, R. *J. Am. Chem. Soc.* **1987**, *109*, 4237.
- (8) Glaser, R.; Choy, G. S.-C.; Hall, M. K. *J. Am. Chem. Soc.* **1991**, *113*, 1109.
- (9) Glaser, R.; Horan, C. J.; Nelson, E.; Hall, M. K. *J. Org. Chem.* **1992**, *57*, 215.
- (10) Glaser, R. *J. Comp. Chem.* **1990**, *11*, 663.
- (11) (a) Lappert, M. F.; Poland, J. S. *J. Chem. Soc., Chem. Commun.* **1969**, 1061. (b) Day, B. W.; George, T. A.; Iske, S. D. *J. Am. Chem. Soc.* **1975**, *97*, 4127. (c) Herrmann, W. A. *Angew. Chem., Int. Ed. Engl.* **1975**, *14*, 355. (d) Hillhouse, G. L.; Haymore, B. L. *Inorg. Chem.* **1979**, *18*, 2423. (e) Herrmann, W. A.; Ziegler, M. L.; Weidenhammer, K. *Angew. Chem., Int. Ed. Engl.* **1976**, *15*, 368.
- (12) The detection of a stable aliphatic C(sp³) connected diazonium ion was claimed recently: Maxwell, J. L.; Brown, K. C.; Bartley, D. W.; Kodadek, T. *Science* **1992**, *256*, 1544.
- (13) Glaser, R.; Chen, G. S.; Barnes, C. L. *Angew. Chem.* **1992**, *104*, 749; *Angew. Chem., Int. Ed. Engl.* **1992**, *31*, 740.
- (14) (a) C₈-N analogue 1-phenylsulfonyl-2-pyrazoline-3-diazonium tetrafluoroborate: Gorelik, M. V.; Tafeenko, V. A.; Rybinov, V. I.; Medvedev, S. V.; Glukhovtsev, M. N. *Zh. Org. Khim.* **1989**, *25*, 2483. (b) C₈-P analogue bis(diisopropylamino)chlorotriphenylmethylidiazomethylenephosphorane hexafluorophosphate: Sotiropoulos, J.-M.; Baccireddo, A.; Horschler von Loquinguin, K.; Dahan, F.; Bertrand, G. *Angew. Chem., Int. Ed. Engl.* **1991**, *30*, 1154; *Angew. Chem.* **1991**, *103*, 1174.
- (15) Reviews: (a) Scherer, O. P. *Angew. Chem., Int. Ed. Engl.* **1985**, *24*, 924. (b) Herrmann, W. A. *Angew. Chem., Int. Ed. Engl.* **1986**, *25*, 56. (c) Vaira, M. D.; Stoppioni, P.; Peruzzini, M. *Polyhedron* **1987**, *6*, 351.
- (16) Niecke, E.; Nieger, M.; Reichert, F.; Schoeller, W. W. *Angew. Chem., Int. Ed. Engl.* **1988**, *27*, 1713.
- (17) Niecke, E.; Nieger, M.; Reichert, F. *Angew. Chem., Int. Ed. Engl.* **1988**, *27*, 1715.
- (18) Glaser, R.; Horan, C. J.; Choy, G. S.-C.; Harris, B. J. *Phys. Chem.* **1992**, *96*, 3689.
- (19) 6-31G* basis set: (a) Hehre, W. J.; Ditchfield, R.; Pople, J. A. *J. Chem. Phys.* **1972**, *56*, 2257. (b) Hariharan, P. C.; Pople, J. A. *Theor. Chim. Acta* **1973**, *28*, 213. (c) Binkley, J. S.; Gordon, J. S.; DeFrees, D. J.; Pople, J. A. *J. Chem. Phys.* **1982**, *77*, 3654. (d) Six Cartesian d-functions were used.
- (20) (a) Krishnan, R.; Binkley, J. S.; Seeger, R.; Pople, J. A. *J. Chem. Phys.* **1980**, *72*, 650. (b) Five pure d- and seven pure f-functions were used with the valence-triple- ζ basis sets.
- (21) (a) *Gaussian90*: Frisch, M. J.; Head-Gordon, M.; Trucks, G. M.; Foresman, J. B.; Schlegel, H. B.; Raghavachari, K.; Robb, M. A.; Binkley, J. S.; Gonzales, C.; Defrees, D. J.; Fox, D. J.; Whiteside, R. A.; Seeger, R.; Melius, C. F.; Baker, J.; Martin, R. L.; Kahn, L. R.; Stewart, J. J. P.; Topiol, S.; Pople, J. A. Gaussian, Inc., Pittsburgh, PA, 1990. (b) Calculations were carried out on a network of Silicon Graphics and Digital Equipment workstations and on an IBM 3090 mainframe with attached FPS processor.
- (22) *CRC Handbook of Chemistry and Physics*, 63rd ed.; CRC Press: Boca Raton, FL, 1985/86; p F-181.
- (23) Structure and frequency of PN : See ref 24, p 564.
- (24) Structure and frequency of P_2 : Huber, K. P.; Herzberg, G. *Constants of Diatomic Molecules*; Van Nostrand Reinhold: New York, 1979.
- (25) Structure and frequencies of N_2 : See ref 24, p 553.
- (26) For near-HF-limit calculations of P_2 see: (a) Mulliken, R. S.; Liu, B. *J. Am. Chem. Soc.* **1971**, *93*, 6738. (b) CI calculations: McLean, A. D.; Liu, B.; Chandler, G. S. *J. Chem. Phys.* **1984**, *80*, 5130.
- (27) Ab initio pseudopotential SCF calculations: (a) Osman, R.; Coffey, P.; Van Wazer, J. R. *Inorg. Chem.* **1976**, *17*, 287. (b) P_n with $n = 2, 4, 8$: Trinquier, G.; Malrieu, J.-P.; Daudey, J.-P. *Chem. Phys. Lett.* **1981**, *80*, 552. (c) P_2 and P_4 : Wedig, U.; Stoll, H.; Preuss, H. *Chem. Phys.* **1981**, *61*, 117.
- (28) For a contrary opinion, see: Brundle, C. R.; Kuebler, N. A.; Robin, N. B.; Basch, H. *Inorg. Chem.* **1972**, *11*, 20.
- (29) Schmidt, M. W.; Gordon, M. S. *Inorg. Chem.* **1985**, *24*, 4503; and references therein.
- (30) For earlier ab initio computations on PN and its protonated ions, see: MacLagan, R. G. A. R. *J. Phys. Chem.* **1990**, *94*, 3373, and references therein.
- (31) A CI study of PN gave the correct equilibrium distance for the ground state: Grein, F.; Kapur, A. *J. Mol. Spectrosc.* **1983**, *99*, 25. Note that their CI energy is higher than the MP4 energies reported here.
- (32) (a) Turner, B. E. *Astrophys. J.* **1974**, *193*, L83. (b) Green, S.; Montgomery, J. A. Thaddeus, P. *Astrophys. J.* **1974**, *193*, L89.
- (33) Olah, G. A.; Herges, R.; Felberg, J. D.; Prakash, G. K. S. *J. Am. Chem. Soc.* **1985**, *107*, 5282.
- (34) Leigh, G. J. *Acc. Chem. Res.* **1992**, *25*, 177.
- (35) HF/6-31G* and MP2/6-31G* calculations of linear 1 were reported: DeFrees, D. J.; McLean, A. D. *J. Chem. Phys.* **1985**, *82*, 333.

- (36) Double- ζ structure of linear 1: Hillier, I. H.; Kendrick, J. *J. Chem. Soc. Chem. Commun.* **1975**, 526.
- (37) For RHF and CISDQ study of the deprotonation of linear 1, see: Kraemer, W. P.; Komornicki, A.; Dixon, D. A. *Chem. Phys.* **1986**, *105*, 87.
- (38) Botschwina, P. *Chem. Phys. Lett.* **1984**, *107*, 535, and references therein.
- (39) Del Bene, J. E.; Frisch, M. J.; Raghavachari, K.; Pople, J. A. *J. Phys. Chem.* **1982**, *86*, 1529.
- (40) Busch, T.; Schoeller, W. W.; Niecke, E.; Nieger, M.; Westermann, H. *Inorg. Chem.* **1989**, *28*, 4334.
- (41) Nguyen, M. T.; Fitzpatrick, N. J. *Chem. Phys. Lett.* **1988**, *146*, 524.
- (42) Maclagan, R. G. A. R. *J. Phys. Chem.* **1990**, *94*, 3373.
- (43) Buenker, R. J.; Bruna, P. J.; Peyerimhoff, S. D. *Isr. J. Chem.* **1980**, *19*, 309.
- (44) Professor Schoeller agrees with our results regarding the shape of the potential energy surface; his more recent MCSCF calculations agree with our CISD results: Private communication at the XIIth ICPC 1992.
- (45) In fact, multiplication of the computed X–Y bond lengths in 1–4 with the appropriate scale factors from Table V results in X–Y bond estimates that differ less than 0.01 Å (and much less in most cases)!
- (46) The differences given are those determined at CISD(full)/6-31G* and the respective values determined at the higher CISD levels are within 10^{-3} .
- (47) (a) Obase, H.; Tsuji, M.; Nishimura, Y. *Chem. Phys. Lett.* **1981**, *81*, 119. (b) Obase, H.; Tsuji, M.; Nishimura, Y. *Chem. Phys.* **1983**, *74*, 89.
- (48) For a comparison of N_2^+ , PN^+ and P_2^+ , see: Grein, F. *Chem. Phys.* **1988**, *120*, 383.
- (49) Compare ref 35.
- (50) Gudemann, C. G.; Begemann, M. H.; Pfaff, J.; Saykally, R. J. *J. Phys. Chem.* **1983**, *78*, 5837.
- (51) Foster, S. C.; McKellar, A. R. W. *J. Chem. Phys.* **1984**, *81*, 3424.
- (52) (a) Komornicki, A.; Pauzat, F.; Ellinger, Y. *J. Phys. Chem.* **1983**, *87*, 3847. (b) See also ref 35. (c) See also ref 37.
- (53) $\Delta\Delta E = -0.600 - 13.508d(\text{NN}) + 0.801d^2(\text{NN})$ with $R^2 = 1.000$.
- (54) $\Delta\Delta E = -53.846 + 16.108d(\text{PP}) - 1.002d^2(\text{PP})$ with $R^2 = 1.000$.
- (55) In fact, the hypothetical protonated systems 1 (2) with an NN (PP) bond length of about 2.0 (1.0) Å, would prefer edge-on (end-on) coordination more than the real system 2 (1).
- (56) Hehre, W. J.; Radom, L.; Schleyer, P. v. R.; Pople, J. A. *Ab Initio Molecular Orbital Theory*; John Wiley: New York, 1986, p 310ff.
- (57) (a) Pullman, A.; Berthod, H.; Gresh, N. *Int. J. Quantum Chem.* **1976**, *10*, 59. (b) Hobza, P.; Zahradnik, R. *Chem. Rev.* **1988**, *88*, 871, and references therein.
- (58) Lias, S. G.; Liebman, J. F.; Levin, R. D. *J. Phys. Chem. Ref. Data* **1984**, *13*, 695.
- (59) (a) 117.4 kcal/mol calculated with highly correlated CEPA level: In ref 38. (b) 119.7 kcal/mol at CISDQ level: In ref 37. (c) 117.8 kcal/mol at MP4/RHF: In ref 39.
- (60) Adams, N. G.; McIntosh, B. J.; Smith, D. *Astronom. Astrophys.* **1990**, *232(2)*, 443.
- (61) On the RHF/6-31G* and MP2/6-31G* potential energy surfaces and at the MP3/6-31G* level based on these structures as well.
- (62) We optimized this structure also at MP2(full)/6-311G(df,p) but did not characterize it via computation of the Hessian matrix.
- (63) Full details of the study of homolytic H–X bond dissociation paths will be described elsewhere. The CISD reaction energies given are size consistency corrected and the VZPE values were used as calculated without scaling.